EAI Endorsed Transactions
on Energy Web
Research Article EAI.EU

Predictive Cross-Layer Anti-Interference Optimization for IoT Data Transmission over Unstable Channels in Power Transmission Environments

Qingdan Huang[1,*], Xihan Xie[1], Dongyi Xiao[1], Haian Ye[1]

[1]Guangdong Power Grid Co., Ltd., Zhanjiang Power Supply Bureau, Zhanjiang, Guangdong, 524000, China

Abstract

INTRODUCTION: Transmission-line Internet of Things (IoT) networks provide continuous sensing for power-grid monitoring, but their wireless links are vulnerable to channel fluctuation, burst interference, sparse relay deployment, and limited node energy.
OBJECTIVES: This paper aims to improve reliable IoT data transmission over unstable transmission-line channels by jointly considering prediction uncertainty, packet urgency, reliability, latency, and energy constraints.
METHODS: A Predictive Cross-layer Anti-interference Optimization (PCAO) method is proposed. PCAO predicts near-future channel and interference states through uncertainty-aware temporal modeling, evaluates packet priority from event severity and information freshness, and jointly optimizes channel allocation, transmission power, redundancy, and relay preference through constrained cross-layer optimization.
RESULTS: Experiments on DeepMIMO, RadioML, POWDER, and FlockLab show that PCAO consistently outperforms DQN, DDPG, PPO, and SAC, improving average packet delivery ratio by 2.55 percentage points over SAC while reducing delay by about 17.0%.
CONCLUSION: The results indicate that predictive, priority-aware, and robust cross-layer control can enhance IoT transmission reliability under unstable channels in power transmission environments.

Received on 4 June 2026; accepted on 24 July 2026; published on 2 September 2026

Keywords: Internet of Things, Power Transmission Environment, Unstable Wireless Channel, Anti-Interference Communication

doi:10.4108/ew.13329

1. Introduction

Transmission-line Internet of Things (IoT) systems are essential for power-grid monitoring, because sensors deployed along towers, conductors, insulators, and corridors continuously collect line temperature, vibration, sag, icing, weather, equipment-status, and abnormal-event data. However, unlike indoor or cellular IoT scenarios, transmission-line environments are geographically open, electromagnetically complex, and operationally unstable. In this paper, “unstable channels” refer to the joint effect of time-varying fading, bursty electromagnetic interference, sparse relay connectivity, weather-induced attenuation, and intermittent obstruction along transmission corridors, rather than a single physical impairment. Wireless links may suffer from rapid channel fluctuation, non-stationary interference, multipath fading, weather-induced attenuation, sparse relay deployment, limited node energy, and intermittent obstruction. Among these factors, the primary technical problem addressed by PCAO is proactive transmission control under uncertain channel–interference evolution, while energy limitation, relay sparsity, and delay constraints are treated as coupled

[*]Corresponding author. Email: huangqing-dan2024@126.com

operational constraints. This makes reliable transmission difficult, especially when urgent monitoring packets require low delay and high reliability. Algorithmically, the key challenge is a coupled cross-layer decision problem involving channel selection, transmission power, redundancy control, routing preference, energy consumption, delay constraint, and packet priority. Existing studies show that learning-based strategies can adapt transmission behavior under wide-area interference [1], RIS-aided receiver architectures can reshape propagation for anti-jamming [2], and edge-assisted collaborative perception can improve robustness in dynamic wireless systems [3]. Nevertheless, transmission-line IoT remains difficult because communication states are partially observable, interference patterns evolve over time, sensing data have different urgency levels, and low-power field nodes cannot support heavy online computation. Therefore, a practical solution should predict unstable channel–interference states, evaluate data importance, and optimize cross-layer transmission actions under constrained resources.

Recent studies have advanced anti-jamming communication from rule-based frequency hopping and static power control toward learning-driven, game-theoretic, and reconfigurable optimization. Learning-based anti-jamming routing improves energy efficiency in dynamic flying ad hoc networks [4], multi-agent reinforcement learning generates personalized anti-interference policies for heterogeneous UAV communication [5], and hierarchical deep reinforcement learning with Transformer-based control supports anti-jamming task scheduling in MEC-O-RAN scenarios [6]. RIS-assisted wireless-powered IoT and compact time-modulated reconfigurable antennas provide infrastructure- and hardware-level anti-jamming solutions [7, 8]. Satellite, multi-agent, distributed, and Stackelberg-game-based studies further extend anti-jamming control to complex wireless settings [9–12]. Physical-layer security, smart-grid worm detection, satellite routing, feedback-free MIMO transmission, and delay-Doppler channel prediction also provide useful foundations for secure, reliable, and predictive wireless communication [13–15]. However, these works still leave three research gaps. First, anti-jamming, routing, physical-layer security, and channel-prediction studies are usually developed as separate modules, so they lack a joint channel–power–redundancy–routing control mechanism for field IoT transmission. Second, most learning-based methods optimize generic throughput, delay, or energy rewards, but they do not explicitly model packet urgency caused by abnormal power-line events, freshness loss, or alarm states. Third, many existing approaches react to the currently observed channel or interference state, but they provide limited uncertainty-aware prediction for proactive decisions before severe packet loss occurs.

To address these gaps, this paper proposes a Predictive Cross-layer Anti-interference Optimization framework, abbreviated as PCAO, for IoT data transmission under unstable transmission-line channels. PCAO is a hybrid learning-assisted optimization framework: the learning component predicts near-future channel and interference states with uncertainty margins, while the optimization component converts these predictions and packet priorities into executable cross-layer transmission decisions. PCAO follows three principles. First, a temporal channel–interference predictor estimates near-future channel quality and interference intensity from historical channel variation, interference variation, queue state, battery level, age of information, and event severity. The predictor is trained from historical transmission-state sequences and is used only to provide predictive state estimates; it does not directly output the final control action. Instead of using only predicted means, PCAO constructs conservative estimates by reducing predicted channel gain and increasing predicted interference according to uncertainty margins. Second, PCAO combines event severity, data freshness, queue pressure, and alarm status into a packet-priority score, so urgent packets receive stronger reliability protection while ordinary packets use more energy-saving policies. Third, PCAO formulates channel allocation, transmission power, redundancy factor, and relay preference as a constrained cross-layer optimization problem covering reliability, delay, energy consumption, and channel occupancy. The nonconvex problem is solved through successive convex approximation and primal–dual updates for edge-assisted deployment. Compared with anti-jamming, RIS-assisted, DRL-based, and routing-oriented methods, PCAO couples prediction, priority modeling, robust estimation, and cross-layer optimization in a single online decision loop. The main contributions are as follows. First, we formulate unstable transmission-line IoT communication as a priority-aware cross-layer anti-interference optimization problem under reliability, delay, energy, and channel-occupancy constraints. Second, we design an uncertainty-aware channel–interference prediction mechanism for proactive transmission control. Third, we develop a constrained optimization algorithm that jointly determines channel allocation, power control, redundancy level, and relay preference. Finally, experiments on four public datasets demonstrate that PCAO improves packet delivery reliability, reduces delay and energy consumption, and achieves stronger anti-interference performance than representative reinforcement-learning baselines.

2. Related Works

Learning-based anti-jamming communication has become a major direction for improving wireless robustness under dynamic interference. Wide-area anti-jamming communication methods have shown that learning-based control can jointly consider energy efficiency and anti-jamming performance, which is highly relevant to low-power IoT transmission [1]. However, their core decision logic is still oriented toward wide-area communication optimization and does not explicitly model packet urgency or transmission-line-specific channel instability. RIS-aided collaborative jamming and anti-jamming networks improve the physical propagation environment through multi-layer transmitting RIS-aided receiver structures, but this type of method depends on additional reconfigurable infrastructure and does not directly solve priority-aware packet scheduling or edge-side cross-layer control [2]. Therefore, PCAO is not intended to replace RIS-assisted or hardware-level anti-jamming techniques; instead, it complements them as a software-level decision-control mechanism that can operate with existing sensing, relay, and edge-computing resources. Edge-assisted collaborative perception has demonstrated that edge nodes can help resist jamming and interference by improving perception and coordination, but its algorithmic focus is perception robustness rather than constrained IoT data-transmission optimization [3]. In contrast, PCAO uses edge-side computation not only to collect communication states, but also to predict future channel–interference conditions and return concrete transmission-control decisions.

Routing-oriented and multi-agent anti-jamming methods provide another important foundation. Learning-based anti-jamming routing with QoS guarantee treats anti-jamming as an adaptive routing problem, which is useful for dynamic topology scenarios [4]. Heterogeneous UAV communication strategies based on multi-agent reinforcement learning further show that personalized anti-interference policies can be generated for different nodes under adversarial wireless conditions [5]. In MEC-O-RAN scenarios, anti-jamming task scheduling has been extended to edge-assisted communication and computation coordination [6]. These studies indicate that intelligent agents can learn robust decisions under adversarial wireless conditions, but they also expose a limitation: the learned action space is usually specialized for routing, scheduling, or local control, while transmission-line IoT requires simultaneous adjustment of channel allocation, power, redundancy, and relay preference. In addition, these methods generally do not incorporate packet-priority modeling driven by event severity and information freshness. PCAO differs from these approaches by formulating the decision as a cross-layer constrained optimization problem rather than a single-layer reinforcement-learning task.

Reconfigurable and physical-layer enhancement methods focus on improving link robustness from the propagation or signal-security perspective. RIS-enhanced wireless-powered IoT networks examine the benefit of RIS for anti-jamming throughput under energy harvesting constraints [7], while time-modulated reconfigurable antennas provide a compact hardware mechanism for anti-jamming IoT communication [8]. DRL-assisted satellite anti-jamming and multi-user collaborative anti-jamming based on discrete soft actor–critic further demonstrate that intelligent control can be integrated with complex wireless environments [9, 10]. These studies are cited only as related evidence that intelligent control and reconfigurable communication can improve robustness under dynamic interference, but their satellite, hardware-assisted, or multi-user adversarial assumptions differ from transmission-line IoT field deployment. However, such approaches either rely on specialized hardware, satellite infrastructure, or multi-user adversarial learning assumptions. Distributed anti-jamming methods based on local knowledge diffusion reduce global information dependence through distributed fusion [11], while Stackelberg-game-based IRS communication confrontation captures the strategic interaction between jammer and defender [12]. These works are valuable but still do not fully address uncertainty-aware prediction and packet-priority modulation. PCAO absorbs the idea of robust anti-jamming control but avoids relying solely on reconfigurable hardware or equilibrium-game assumptions.

Physical-layer security and grid-oriented security studies address another side of reliable communication. Robust grant-free mMTC security improves secure access in massive machine-type communication [13], and learning-based friendly jamming under imperfect CSI enhances MIMO wiretap-channel security [14]. These works are relevant as robustness-oriented wireless studies, but their main missing capability relative to PCAO is the absence of packet-level reliability-delay-energy coordination for operational monitoring traffic. These studies are important for communication confidentiality and robustness, but their objectives differ from the operational reliability problem in transmission-line IoT, where urgent monitoring packets must be delivered under delay and energy constraints. Reinforcement-learning-based worm detection for smart grids is closer to the power-system context, but it mainly focuses on cyberattack detection rather than wireless transmission control [15]. Therefore, PCAO complements these studies by targeting transmission reliability and anti-interference optimization rather than only secure access or attack detection.

Reliable routing and predictive channel modeling are also related to the proposed framework. Multi-agent reliable routing for VLEO satellite optical networks and DRL-based multipath cooperative routing in ultradense LEO satellite networks show that learning-based routing can improve reliability under highly dynamic network conditions [16, 17]. Feedback-free MIMO transmission reduces dependence on explicit channel feedback, which is relevant when transmission-line IoT links have incomplete or delayed feedback [18]. Delay-Doppler domain channel prediction using large AI models further shows that predictive modeling can support proactive wireless transmission decisions [19]. However, these studies mainly contribute routing reliability, feedback reduction, or channel prediction, whereas PCAO requires the prediction result to be coupled with packet priority, power allocation, redundancy control, and relay preference in one constrained decision loop. Nevertheless, these methods are usually designed for satellite, MIMO, or vehicular communication systems, and their optimization targets do not include the packet-priority and energy-limited characteristics of field-deployed IoT sensors. PCAO therefore extends predictive communication control to the transmission-line IoT setting by combining temporal channel–interference prediction, conservative robust estimation, priority-aware utility design, and constrained cross-layer optimization. This makes the proposed method different from existing anti-jamming, routing, physical-layer security, and channel-prediction studies, because it treats unstable communication as a unified algorithmic decision problem rather than a set of isolated subproblems.

3. Methodology

To address unreliable wireless links, burst interference, limited node energy, and priority-sensitive data transmission in transmission-line Internet of Things (IoT) environments, this paper proposes a *Predictive Cross-layer Anti-interference Optimization* framework, abbreviated as **PCAO**. The central idea is to combine channel–interference prediction, packet-priority evaluation, and constrained cross-layer transmission optimization into a unified online decision process. Unlike reactive schemes that adjust communication parameters only after link degradation or packet loss occurs, PCAO predicts near-future channel and interference states, evaluates the operational importance of packets, and jointly optimizes channel allocation, transmission power, redundancy level, and relay preference. The overall workflow is shown in Fig. 1. The online deployment and convergence process are further illustrated in Fig. 2.

3.1. System Model and Optimization Objective

We consider a transmission-line IoT network represented by a directed graph

$$\mathcal{G} = (\mathcal{V}, \mathcal{E}), \tag{1}$$

where $\mathcal{V} = \{1, 2, \dots, M\}$ denotes the set of sensing or relay nodes deployed along transmission towers, insulators, conductors, and corridor monitoring points, and $\mathcal{E}$ denotes the set of feasible wireless links. Time is divided into discrete slots indexed by t.

At time slot t, node i observes a local communication-state vector

$$\mathbf{o}_i^t = \left[h_i^t,\ j_i^t,\ \Delta h_i^t,\ \Delta j_i^t,\ q_i^t,\ b_i^t,\ a_i^t,\ \delta_i^t\right]^\top, \tag{2}$$

where h_i^t is the measured channel-quality indicator, j_i^t is the observed interference intensity, Δh_i^t and Δj_i^t are the short-term variations of channel quality and interference intensity, q_i^t is the queue length, b_i^t is the residual battery level, a_i^t is the age of information, and δ_i^t is the event-severity score extracted from the sensed data.

The cross-layer action of node i is defined as

$$\mathbf{z}_i^t = \left[x_{i,1}^t, \dots, x_{i,N}^t,\ p_i^t,\ \kappa_i^t,\ y_{i,1}^t, \dots, y_{i,M}^t\right]^\top, \tag{3}$$

where $x_{i,n}^t$ denotes the allocation ratio of channel n and is used as a relaxed channel-selection score during optimization, p_i^t is the transmission power, κ_i^t is the redundancy factor for coding or retransmission enhancement, and $y_{i,j}^t$ denotes the routing preference from node i to next-hop node j and is used as a relaxed next-hop score. For online tractability, channel selection and routing are relaxed into continuous variables:

$$\begin{aligned} &\sum_{n=1}^{N} x_{i,n}^t = 1, \qquad \sum_{j=1}^{M} y_{i,j}^t = 1, \\ &0 \le p_i^t \le P_i^{\max}, \qquad 1 \le \kappa_i^t \le \kappa_{\max}. \end{aligned} \tag{4}$$

The relaxed variables in (3) and (4) are used only inside the optimizer to make the cross-layer problem tractable. During real deployment, they are converted into executable discrete decisions before transmission. Specifically, the edge controller treats $x_{i,n}^t$ as the priority score of assigning channel n to node i and selects the channel with the largest feasible score, while respecting the channel-occupancy constraint $\sum_i x_{i,n}^t \le 1$. If two nodes prefer the same channel, the conflict is resolved according to the priority-weighted score $\pi_i^t x_{i,n}^t$ and the remaining nodes are assigned to the next-best available channels. Similarly, $y_{i,j}^t$ is converted into a next-hop decision by selecting the feasible neighbor with the largest routing score among $(i, j) \in \mathcal{E}$; if the selected relay violates delay, energy, or connectivity

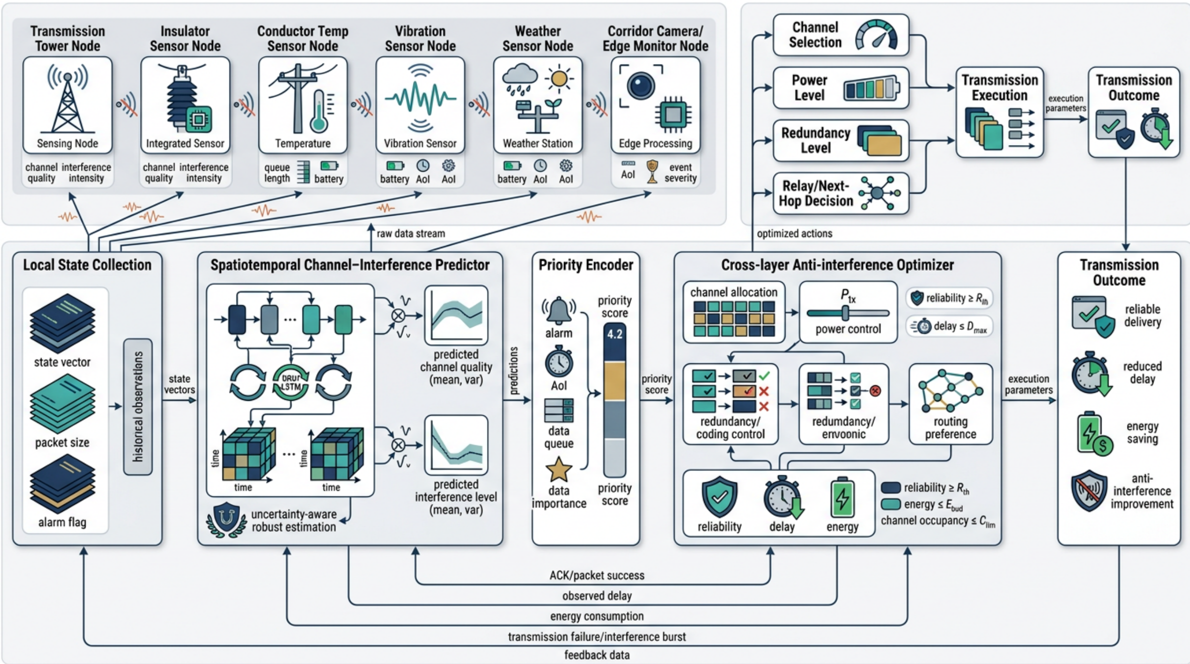

Figure 1. Overall workflow of the proposed PCAO framework. Transmission-line IoT nodes collect sensing data and communication states, after which the channel–interference predictor estimates near-future link conditions with uncertainty awareness. The priority encoder evaluates packet urgency, and the cross-layer optimizer determines channel allocation, power control, redundancy level, and relay preference. The transmission outcomes are fed back for online refinement

constraints, the next highest-ranked feasible relay is used. The power variable is clipped or quantized to the supported radio power level, and κ_i^t is rounded to the nearest supported coding or retransmission level. Therefore, the deployed action is a discrete channel index, a hardware-supported power level, a discrete redundancy setting, and a single next-hop relay, rather than a fractional transmission action.

The robust signal-to-interference-plus-noise ratio (SINR) of node i on channel n is modeled as

$$\gamma_{i,n}^t = \frac{x_{i,n}^t p_i^t \bar{h}_{i,n}^{t+1}}{N_0 B_n + \bar{j}_{i,n}^{t+1} + \sum_{k\neq i} x_{k,n}^t p_k^t \bar{g}_{k,i,n}^{t+1}}, \tag{5}$$

where N_0 is the noise spectral density, B_n is the bandwidth of channel n, $\bar{h}_{i,n}^{t+1}$ is the predicted robust channel gain, $\bar{j}_{i,n}^{t+1}$ is the predicted interference level, and $\bar{g}_{k,i,n}^{t+1}$ represents the co-channel coupling effect from node k to node i.

The achievable transmission rate is

$$R_i^t = \sum_{n=1}^{N} B_n \log_2\left(1 + \gamma_{i,n}^t\right). \tag{6}$$

The packet delivery reliability is approximated by

$$\psi_i^t = 1 - \exp\left(-\nu_i \kappa_i^t \sum_{n=1}^{N} \gamma_{i,n}^t\right), \tag{7}$$

where $\nu_i > 0$ is a modulation-dependent shaping coefficient. This formulation reflects that higher SINR and stronger redundancy generally improve delivery probability under unstable channels. The exponential form is adopted as a bounded and monotonic packet-success surrogate. It can be interpreted as the complement of an outage or residual-error probability that decreases approximately exponentially with effective SINR and diversity/retransmission gain. This choice also avoids an over-complex bit-error-rate expression for every modulation and coding scheme, while preserving the required properties $\psi_i^t \in [0, 1]$, $\partial\psi_i^t/\partial\gamma_{i,n}^t > 0$, and $\partial\psi_i^t/\partial\kappa_i^t > 0$. The shaping coefficient ν_i is calibrated offline for each radio configuration by fitting the surrogate reliability curve to empirical ACK ratios or link-level simulation results under the corresponding modulation, coding rate, packet length, and retransmission limit. In implementation, a lookup table of ν_i can be maintained for different MCS and retransmission settings, and the redundancy factor κ_i^t captures the additional reliability gain from coding or repeated transmission.

The delay and energy consumption of node i are respectively defined as

$$D_i^t = \frac{L_i^t}{R_i^t} + \sum_{j=1}^{M} y_{i,j}^t \tau_{i,j} + (\kappa_i^t - 1)\tau_r, \tag{8}$$

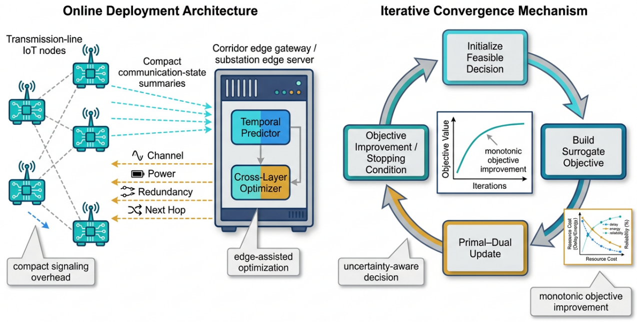

Figure 2. Online deployment and convergence process of PCAO

and

$$E_i^t = p_i^t \frac{L_i^t}{R_i^t} + \epsilon_c(\kappa_i^t - 1), \tag{9}$$

where L_i^t is the packet size, $\tau_{i,j}$ is the forwarding delay from node i to node j, τ_r is the delay overhead caused by redundancy, and ϵ_c is the additional energy cost of coding or retransmission.

The long-term objective is to maximize priority-weighted reliable transmission utility while controlling delay and energy consumption:

$$\max_{\{\mathbf{z}_i^t\}} \liminf_{T\to\infty} \frac{1}{T}\mathbb{E}\left[\sum_{t=1}^{T}\sum_{i=1}^{M}\left(\pi_i^t\psi_i^t - \lambda_D D_i^t - \lambda_E E_i^t\right)\right], \tag{10}$$

where π_i^t is the packet-priority score, while λ_D and λ_E are nonnegative penalty coefficients for delay and energy.

The optimization is subject to the following reliability, delay, energy, and channel-occupancy constraints:

$$\begin{aligned}
&\limsup_{T\to\infty} \frac{1}{T}\sum_{t=1}^{T}\mathbb{E}[E_i^t] \le \bar{E}_i,\\
&\limsup_{T\to\infty} \frac{1}{T}\sum_{t=1}^{T}\mathbb{E}[D_i^t] \le \bar{D}_i,\\
&\liminf_{T\to\infty} \frac{1}{T}\sum_{t=1}^{T}\mathbb{E}[\psi_i^t] \ge \bar{\Psi}_i,\\
&\sum_{i=1}^{M} x_{i,n}^t \le 1, \qquad \forall n,t.
\end{aligned} \tag{11}$$

3.2. Channel–Interference Prediction and Packet Priority Modeling

Transmission-line environments contain burst electromagnetic interference, weather-induced attenuation, multipath fading, and intermittent obstruction. Therefore, PCAO does not directly optimize actions based only on current observations. Instead, it predicts near-future channel and interference states and then performs robust decision-making.

For each node i, a temporal encoder maintains a latent communication representation:

$$\mathbf{s}_i^t = \mathrm{GRU}_\phi\left(\mathbf{s}_i^{t-1}, \mathbf{o}_i^t\right), \tag{12}$$

where ϕ denotes the trainable parameters of the gated recurrent unit.

The prediction head estimates both the mean and uncertainty of the next-slot channel and interference conditions:

$$\left[\mu_{i,h}^{t+1}, \log(\sigma_{i,h}^{t+1})^2, \mu_{i,j}^{t+1}, \log(\sigma_{i,j}^{t+1})^2\right] = \mathbf{W}_p\mathbf{s}_i^t + \mathbf{b}_p, \tag{13}$$

where $\mu_{i,h}^{t+1}$ and $\mu_{i,j}^{t+1}$ are predicted means, while $\sigma_{i,h}^{t+1}$ and $\sigma_{i,j}^{t+1}$ represent predictive uncertainty.

To avoid aggressive decisions under uncertain conditions, PCAO uses conservative robust estimates:

$$\tilde{h}_i^{t+1} = \mu_{i,h}^{t+1} - \xi_h\sigma_{i,h}^{t+1}, \qquad \tilde{j}_i^{t+1} = \mu_{i,j}^{t+1} + \xi_j\sigma_{i,j}^{t+1}, \tag{14}$$

where ξ_h and ξ_j are uncertainty margins. Thus, the optimizer assumes a pessimistic channel gain and a stronger possible interference level, which improves robustness in highly unstable environments.

The prediction module is trained by minimizing the Gaussian negative log-likelihood:

$$\begin{aligned}
\mathcal{L}_{\mathrm{pred}} = \sum_{i,t}\Bigg[&\frac{(h_i^{t+1}-\mu_{i,h}^{t+1})^2}{2(\sigma_{i,h}^{t+1})^2} + \log\sigma_{i,h}^{t+1}\\
&+ \frac{(j_i^{t+1}-\mu_{i,j}^{t+1})^2}{2(\sigma_{i,j}^{t+1})^2} + \log\sigma_{i,j}^{t+1}\Bigg].
\end{aligned} \tag{15}$$

In addition to communication-state prediction, PCAO evaluates the operational importance of packets. The packet-priority score is defined as

$$\pi_i^t = \omega_1\delta_i^t + \omega_2\frac{a_i^t}{a_{\max}} + \omega_3\frac{q_i^t}{q_{\max}} + \omega_4\chi_i^t, \tag{16}$$

where χ_i^t is an alarm flag, and $\omega_1, \omega_2, \omega_3, \omega_4 \ge 0$ with $\sum_{m=1}^{4}\omega_m = 1$. This design ensures that urgent, stale, queued, or alarm-related packets receive stronger reliability protection during transmission optimization. The weights are not treated as trainable neural parameters. They are selected through a domain-guided validation procedure: event severity and alarm status are assigned higher priority because they correspond to safety-critical line conditions, while age of information and queue length are used to avoid stale-data accumulation and buffer congestion. Candidate weight vectors satisfying $\sum_{m=1}^{4}\omega_m = 1$ are evaluated on the validation set, and the setting with the best priority-weighted reliability–delay–energy trade-off is used for testing. To examine sensitivity, the weights can be perturbed around the selected configuration while keeping the same normalization constraint; stable performance under these perturbations indicates that PCAO depends mainly on the priority ordering rather than on one exact manual weight value.

3.3. Priority-Aware Cross-Layer Anti-interference Optimization

The original problem is non-convex because channel allocation, power control, co-channel interference, redundancy, and routing are mutually coupled through the SINR, rate, delay, and reliability terms. PCAO solves this problem using a successive convex approximation strategy combined with primal–dual updates.

Let $\mathbf{z}^t = \{\mathbf{z}_i^t\}_{i=1}^M$ denote the global decision variable. At outer iteration m, PCAO constructs a locally tight surrogate objective around the current feasible point $\mathbf{z}^{(m)}$:

$$\hat{F}(\mathbf{z} \mid \mathbf{z}^{(m)}) = \sum_{i=1}^{M} \left(\pi_i \hat{\psi}_i - \lambda_D \hat{D}_i - \lambda_E \hat{E}_i\right) - \frac{\rho}{2}\|\mathbf{z} - \mathbf{z}^{(m)}\|_2^2. \tag{17}$$

where $\hat{\psi}_i$, $\hat{D}_i$, and $\hat{E}_i$ are first-order local approximations of reliability, delay, and energy, and $\rho > 0$ is a proximal coefficient used to stabilize the update.

The surrogate is required to satisfy

$$\begin{aligned} \hat{F}(\mathbf{z}^{(m)} \mid \mathbf{z}^{(m)}) &= F(\mathbf{z}^{(m)}), \\ \nabla\hat{F}(\mathbf{z}^{(m)} \mid \mathbf{z}^{(m)}) &= \nabla F(\mathbf{z}^{(m)}). \end{aligned} \tag{18}$$

These two conditions ensure that the surrogate objective is locally consistent with the original objective.

The constrained surrogate problem is written as

$$\max_{\mathbf{z}\in\mathcal{Z}} \hat{F}(\mathbf{z} \mid \mathbf{z}^{(m)}), \tag{19}$$

where $\mathcal{Z}$ denotes the feasible set defined by channel assignment, power, redundancy, routing, reliability, delay, and energy constraints.

To solve this problem in an edge-assisted distributed manner, the Lagrangian is formulated as

$$\begin{aligned} \mathcal{L} =& \hat{F} - \sum_{n=1}^{N} \alpha_n \left(\sum_{i=1}^{M} x_{i,n} - 1\right) \\ &- \sum_{i=1}^{M} \beta_i (E_i - \bar{E}_i) - \sum_{i=1}^{M} \mu_i (D_i - \bar{D}_i). \end{aligned} \tag{20}$$

where α_n, β_i, and μ_i are nonnegative dual variables for channel occupancy, energy budget, and delay constraints.

The primal variables are updated by projected gradient ascent:

$$\mathbf{g}_i^{(\ell)} = \nabla_{\mathbf{z}_i} \mathcal{L}\left(\mathbf{z}^{(\ell)}, \boldsymbol{\alpha}^{(\ell)}, \boldsymbol{\beta}^{(\ell)}, \boldsymbol{\mu}^{(\ell)}\right). \tag{21}$$

$$\mathbf{z}_i^{(\ell+1)} = \Pi_{\mathcal{Z}_i}\left[\mathbf{z}_i^{(\ell)} + \eta_z \mathbf{g}_i^{(\ell)}\right]. \tag{22}$$

where $\Pi_{\mathcal{Z}_i}(\cdot)$ is Euclidean projection onto the local feasible set and η_z is the primal step size.

The dual variables are updated as

$$\begin{aligned} \alpha_n^{(\ell+1)} &= \left[\alpha_n^{(\ell)} + \eta_\alpha \left(\sum_{i=1}^{M} x_{i,n}^{(\ell+1)} - 1\right)\right]_+, \\ \beta_i^{(\ell+1)} &= \left[\beta_i^{(\ell)} + \eta_\beta \left(E_i^{(\ell+1)} - \bar{E}_i\right)\right]_+, \\ \mu_i^{(\ell+1)} &= \left[\mu_i^{(\ell)} + \eta_\mu \left(D_i^{(\ell+1)} - \bar{D}_i\right)\right]_+. \end{aligned} \tag{23}$$

The priority score π_i^t directly adjusts the optimizer's preference. When π_i^t is high, the utility term places greater emphasis on packet reliability, allowing the optimizer to allocate more favorable channels, higher redundancy, or stronger transmission power. When π_i^t is low, the optimizer tends to choose more energy-saving decisions. In this way, PCAO realizes adaptive trade-off control among reliability, latency, and energy consumption.

3.4. Distributed Algorithm, Deployment, and Convergence Analysis

The online implementation of PCAO is summarized in Algorithm 1. The sensing nodes collect local communication states and packet metadata, while the edge gateway performs prediction and cross-layer optimization. Only compact state summaries and control variables are exchanged, which makes the method suitable for resource-constrained transmission-line IoT systems.

Theorem 1. Assume that the feasible set $\mathcal{Z}$ is nonempty, closed, and compact, and that the original objective function is continuously differentiable on $\mathcal{Z}$. If the surrogate objective in (17) satisfies the local consistency condition in (18) and is solved exactly or with bounded optimization error at each outer iteration, then the sequence generated by PCAO converges to a stationary solution of the original constrained optimization problem.

Proof. At iteration m, the next solution $\mathbf{z}^{(m+1)}$ is obtained by maximizing the surrogate objective. Therefore,

$$\hat{F}(\mathbf{z}^{(m+1)} \mid \mathbf{z}^{(m)}) \geq \hat{F}(\mathbf{z}^{(m)} \mid \mathbf{z}^{(m)}). \tag{24}$$

Because the surrogate is locally tight at $\mathbf{z}^{(m)}$, we have

$$\hat{F}(\mathbf{z}^{(m)} \mid \mathbf{z}^{(m)}) = F(\mathbf{z}^{(m)}). \tag{25}$$

With the proximal regularization term, the update remains stable and prevents unbounded oscillation

Algorithm 1 Predictive Cross-layer Anti-interference Optimization

Require: Historical observations, initial predictor parameter ϕ, feasible initial decision $\mathbf{z}^{(0)}$

```
for each time slot t = 1, 2, ... do
    for each node i ∈ V do
        Collect local observation o_i^t and packet metadata (L_i^t, δ_i^t, χ_i^t)
        Update latent state s_i^t using (12)
        Predict channel and interference statistics using (13)
        Compute robust estimates using (14)
        Compute packet-priority score using (16)
    end for
    Initialize SCA iteration index m = 0
    repeat
        Construct surrogate objective using (17)
        repeat
            Update primal variables using (22)
            Update dual variables using (23)
        until inner primal–dual iteration converges
        Update z^(m+1) by solving (19)
        m ← m + 1
    until objective improvement is smaller than ε
    Convert relaxed channel-allocation and routing-preference variables into discrete channel-selection and next-hop-routing decisions
    Execute channel, power, redundancy, and relay decisions
    Observe ACK, delay, energy, and packet outcome
    Update predictor parameter φ using (15)
end for
```

between consecutive iterates. Since $\mathcal{Z}$ is compact and $F(\mathbf{z})$ is continuous, the objective sequence is bounded. Hence, the monotonic or sufficiently descent-controlled improvement sequence converges.

Let $\bar{\mathbf{z}}$ be an accumulation point of $\{\mathbf{z}^{(m)}\}$. The first-order optimality condition of the surrogate problem holds at the limit point. Due to the gradient consistency condition in (18), the limiting first-order condition of the surrogate problem is also the first-order stationarity condition of the original problem. The projected dual updates in (23) enforce feasibility and complementary slackness for channel occupancy, delay, and energy constraints. Therefore, $\bar{\mathbf{z}}$ satisfies the Karush–Kuhn–Tucker stationary condition of the original constrained problem. This proves the convergence of PCAO to a stationary solution. ■

The computational complexity of PCAO is mainly determined by the temporal predictor and the iterative optimizer. Let d_s denote the GRU hidden dimension, M the number of nodes, N the number of channels, I_{out} the number of SCA iterations, and I_{in} the number of primal–dual iterations. The per-slot complexity is approximately

$$\mathcal{O}\left(Md_s^2 + I_{\text{out}}I_{\text{in}}M(N+M)\right). \tag{26}$$

This complexity is acceptable for edge-assisted execution because low-power IoT nodes only perform sensing and state reporting, while prediction, optimization, and control generation are executed at the transmission-corridor edge gateway or substation-side computing unit.

In practical deployment, PCAO requires each node to upload only compact communication-state summaries, including channel quality, interference intensity, queue length, battery level, and packet urgency indicators. The edge gateway returns a lightweight control tuple consisting of a discrete channel index, a supported power level, a discrete redundancy level, and a selected next-hop relay. This design avoids heavy local computation at field-deployed IoT nodes and enables reliable transmission under unstable channels, burst interference, and energy-constrained operating conditions.

4. Experiment

4.1. Experimental setup

All experiments were conducted on a workstation equipped with an Intel Core i9-12900K CPU, 64 GB RAM, a 2 TB NVMe SSD, and one NVIDIA RTX 3090 GPU with 24 GB memory. The software environment was Ubuntu 22.04 LTS, Python 3.10, PyTorch 2.2, CUDA 12.1, cuDNN 8.9, NumPy 1.26, pandas 2.2, scikit-learn 1.4, and Matplotlib 3.8. To evaluate the proposed PCAO method under heterogeneous unstable-channel and interference conditions, four public datasets were used: DeepMIMO for ray-tracing-based MIMO channel modeling and spatially dependent channel variation [20], RadioML 2016.10A for radio signal samples with multiple modulation types and varying signal-to-noise ratios [21, 22], POWDER Data Commons interference traces for receiver I/Q samples under 0–4 simultaneous OFDM interferers, and the FlockLab wireless link-quality dataset for low-power wireless link estimation using empirical packet-level traces [23]. To transform these heterogeneous datasets into the same transmission-control task, all raw records were converted into slot-level samples with a unified state–action–outcome format. Specifically, dataset-specific measurements were mapped to the common communication-state variables in Eq. (2), including channel quality, interference intensity, short-term channel/interference variation, queue state, residual energy, age of information, and event severity. DeepMIMO mainly provides channel-gain and spatial-link variation, RadioML provides signal-level SNR and modulation-dependent disturbance information,

Table 1. Overall transmission performance comparison on four public datasets

Dataset	Method	PDR (%) ↑	Throughput (Mbps) ↑	Delay (ms) ↓	Energy (mJ/packet) ↓	PLR (%) ↓	SINR Gain (dB) ↑	ISG (dB) ↑
DeepMIMO	DQN	88.4	6.91	24.8	3.72	11.6	4.36	3.91
	DDPG	91.2	7.35	21.3	3.41	8.8	5.14	4.48
	PPO	92.6	7.68	19.4	3.18	7.4	5.73	4.92
	SAC	94.7	8.21	17.6	2.91	5.3	6.48	5.61
	PCAO	**96.8**	**8.73**	**14.2**	**2.54**	**3.2**	**7.82**	**6.47**
RadioML	DQN	86.9	5.82	27.1	3.89	13.1	3.94	3.42
	DDPG	89.7	6.34	23.6	3.53	10.3	4.76	4.11
	PPO	91.5	6.71	21.8	3.31	8.5	5.21	4.58
	SAC	93.1	7.06	19.5	3.04	6.9	5.88	5.16
	PCAO	**95.9**	**7.64**	**16.7**	**2.68**	**4.1**	**7.13**	**6.02**
POWDER	DQN	84.3	5.47	31.6	4.26	15.7	3.61	3.24
	DDPG	87.5	5.96	28.4	3.91	12.5	4.33	3.86
	PPO	89.4	6.28	25.9	3.64	10.6	4.92	4.39
	SAC	92.2	6.86	22.3	3.28	7.8	5.81	5.27
	PCAO	**95.2**	**7.41**	**18.1**	**2.87**	**4.8**	**7.36**	**6.94**
FlockLab	DQN	85.8	4.92	29.3	3.54	14.2	3.38	3.07
	DDPG	88.6	5.38	26.1	3.21	11.4	4.02	3.71
	PPO	90.3	5.76	23.8	2.98	9.7	4.61	4.26
	SAC	92.5	6.24	21.2	2.73	7.5	5.37	4.93
	PCAO	**94.8**	**6.82**	**17.9**	**2.31**	**5.2**	**6.69**	**5.88**

POWDER provides explicit multi-interferer traces and receiver I/Q-derived interference intensity, and FlockLab provides empirical RSSI/LQI, packet reception, and low-power link-quality fluctuation. When queue length, battery state, or packet urgency was not directly available, it was generated by the same trace-driven simulator using packet-arrival rate, transmission outcome, freshness, and abnormal-link-event indicators. Therefore, each dataset was finally evaluated as the same online decision problem: given the current and predicted communication state, the controller selects channel, power, redundancy, and relay decisions and is evaluated by packet delivery, delay, energy, and anti-interference metrics. For each dataset, the chronological records were divided into 70% training, 15% validation, and 15% testing subsets to avoid temporal leakage. The input features included channel quality indicators, RSSI/SINR-related measurements, interference intensity, packet reception information, queue state, packet urgency, and normalized energy state when available. Four baseline algorithms were compared with PCAO: DQN, which learns discrete channel and routing decisions through value approximation [24]; DDPG, which optimizes continuous transmission-control variables such as power and redundancy under deterministic policy gradients [25]; PPO, which uses clipped policy optimization for stable cross-layer action learning [26]; and SAC, which introduces entropy-regularized actor–critic learning for robust continuous control in uncertain environments [27]. All learning-based methods used the same transformed transmission-control task, observation space, training/validation/testing split, maximum training episodes, and random seeds for fair comparison. The evaluation metrics included packet delivery ratio (PDR), average end-to-end delay, normalized throughput, energy consumption per successfully delivered packet, packet loss rate, average SINR improvement, interference suppression gain, reliability-constraint violation ratio, and channel–interference prediction error measured by MAE and RMSE. These metrics jointly evaluate whether the proposed method can improve reliable data delivery, reduce latency and energy consumption, and maintain robust transmission performance under unstable channels and dynamic interference.

4.2. Overall Transmission Performance Comparison

This experiment evaluates the overall transmission performance of the proposed PCAO method against four reinforcement-learning-based baselines, namely DQN, DDPG, PPO, and SAC. The comparison is conducted on four datasets, including DeepMIMO, RadioML, POWDER, and FlockLab, to cover different unstable-channel and interference conditions. DeepMIMO mainly reflects spatially varying wireless channels, RadioML provides signal-level variations under different noise conditions, POWDER emphasizes multi-interferer wireless environments, and FlockLab represents empirical low-power wireless link-quality fluctuations. Seven metrics are adopted for comprehensive evaluation: packet delivery ratio (PDR), throughput, delay, energy consumption per successfully delivered packet, packet loss rate (PLR), SINR gain, and interference suppression gain (ISG). The overall transmission performance comparison is reported in Table 1, while the ablation results are separately reported in Table 2. This distinction is used to keep the table numbering, captions, and discussion consistent.

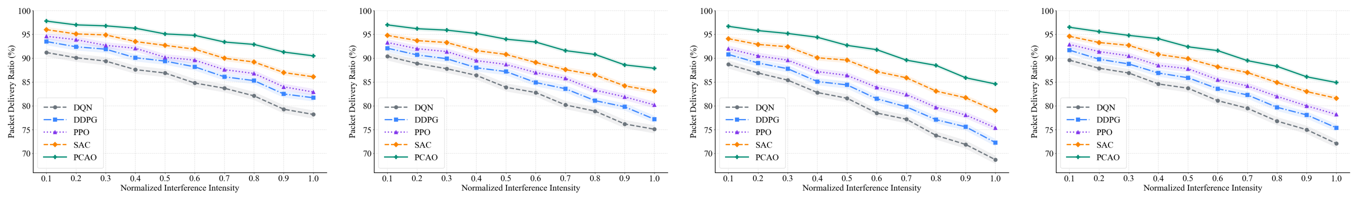

(a) DeepMIMO (b) RadioML (c) POWDER (d) FlockLab

Figure 3. Packet delivery ratio comparison under increasing normalized interference intensity on four datasets.

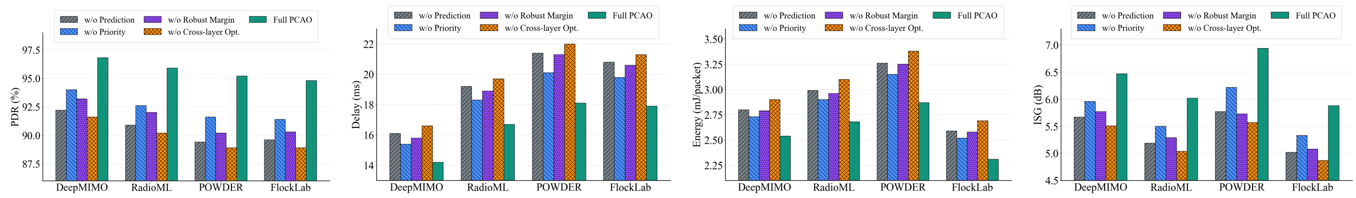

(a) PDR comparison. (b) Delay comparison. (c) Energy comparison. (d) ISG comparison.

Figure 4. Ablation study of PCAO components on four datasets

As shown in Table 1, PCAO achieves the best results on all four datasets across all seven metrics, indicating its stable advantage under different unstable-channel and interference conditions. On DeepMIMO, PCAO reaches 96.8% PDR, 8.73 Mbps throughput, and 14.2 ms delay, showing strong adaptability to spatially varying channel conditions. On RadioML, PCAO improves PDR to 95.9% and reduces PLR to 4.1%, suggesting that the uncertainty-aware prediction module can effectively handle signal-level noise and modulation variations. On POWDER, PCAO obtains the largest anti-interference advantage, with 7.36 dB SINR gain and 6.94 dB ISG, which confirms its effectiveness under multi-interferer wireless environments. On FlockLab, PCAO achieves the lowest energy consumption of 2.31 mJ/packet while maintaining 94.8% PDR, demonstrating its suitability for low-power IoT deployment. The reported average improvements are computed as arithmetic averages over the four dataset-level test results in Table 1, rather than over all interference-intensity points in Fig. 3. They are calculated against SAC only, because SAC has the strongest average performance among the four baselines in Table 1. Under this calculation, PCAO improves the average PDR from 93.13% to 95.68%, namely by 2.55 percentage points; increases the average throughput from 7.09 Mbps to 7.65 Mbps, namely by 0.56 Mbps; and reduces the average delay from 20.15 ms to 16.73 ms, corresponding to an approximate 17.0% reduction. These results verify that the proposed combination of channel–interference prediction, packet-priority modeling, robust estimation, and cross-layer optimization can achieve a better trade-off among reliability, latency, energy efficiency, and anti-interference performance.

4.3. Robustness under Increasing Interference Intensity

This experiment evaluates the robustness of PCAO and the baseline methods under gradually increasing interference intensity. The objective is to verify whether the proposed method can maintain a higher packet delivery ratio when the wireless environment becomes increasingly unstable and interference-dominant.

As shown in Fig. 3, the packet delivery ratio of all methods decreases as the normalized interference intensity increases, which confirms that stronger interference directly weakens wireless transmission reliability. However, PCAO consistently maintains the highest PDR on all four datasets and shows a slower degradation trend than DQN, DDPG, PPO, and SAC. More specifically, at the most severe interference point on the right side of each curve, PCAO still remains above the closest baseline, which is usually SAC. The degradation of PCAO from the low-interference region to the highest-interference region is visually smaller than that of the baselines, generally staying within a moderate PDR loss range, whereas DQN and DDPG show much sharper drops. The gap is most evident on POWDER, where the multi-interferer traces cause the baseline curves to decline more rapidly, while PCAO preserves a visibly higher terminal PDR. On DeepMIMO and RadioML, PCAO preserves a clear advantage under both moderate and severe interference, indicating that its channel–interference prediction module can capture unstable signal variations before transmission decisions are made. On POWDER, where multi-interferer conditions are more explicit,

Table 2. Ablation study of PCAO components on four datasets

Dataset	Variant	PDR (%) ↑	Delay (ms) ↓	Energy (mJ/packet) ↓	ISG (dB) ↑
DeepMIMO	w/o Prediction	92.2	16.1	2.80	5.67
	w/o Priority	94.0	15.4	2.73	5.96
	w/o Robust Margin	93.2	15.8	2.79	5.77
	w/o Cross-layer Opt.	91.6	16.6	2.90	5.51
	Full PCAO	**96.8**	**14.2**	**2.54**	**6.47**
RadioML	w/o Prediction	90.9	19.2	2.99	5.19
	w/o Priority	92.6	18.3	2.90	5.50
	w/o Robust Margin	92.0	18.9	2.96	5.29
	w/o Cross-layer Opt.	90.2	19.7	3.10	5.04
	Full PCAO	**95.9**	**16.7**	**2.68**	**6.02**
POWDER	w/o Prediction	89.4	21.4	3.26	5.77
	w/o Priority	91.6	20.1	3.15	6.22
	w/o Robust Margin	90.2	21.3	3.25	5.73
	w/o Cross-layer Opt.	88.9	22.0	3.38	5.57
	Full PCAO	**95.2**	**18.1**	**2.87**	**6.94**
FlockLab	w/o Prediction	89.6	20.8	2.59	5.02
	w/o Priority	91.4	19.8	2.52	5.33
	w/o Robust Margin	90.3	20.6	2.58	5.08
	w/o Cross-layer Opt.	88.9	21.3	2.69	4.87
	Full PCAO	**94.8**	**17.9**	**2.31**	**5.88**

the performance gap between PCAO and the baselines becomes more evident, showing that robust interference estimation and redundancy-aware control are effective for interference-dominant environments. On FlockLab, PCAO also remains superior under empirical low-power wireless link fluctuations, which suggests that the proposed method is suitable for resource-constrained IoT deployment rather than only simulated channels. The main reason for PCAO's advantage is that it does not rely on a single reactive control policy; instead, it jointly combines uncertainty-aware channel prediction, packet-priority modeling, robust margin estimation, and cross-layer optimization of channel allocation, power, redundancy, and relay preference. Therefore, when interference becomes stronger, PCAO can proactively select more reliable channels, adjust transmission power and redundancy, and avoid unstable forwarding paths, leading to a more stable PDR curve across heterogeneous datasets.

4.4. Ablation Study of PCAO Components

This experiment evaluates the contribution of each core component in PCAO, including channel–interference prediction, packet-priority modeling, robust margin estimation, and cross-layer joint optimization. Four ablated variants are compared with the full PCAO model on all datasets to verify whether each module contributes to reliable, low-latency, energy-efficient, and interference-resistant transmission. The four variants are defined as follows. "w/o Prediction" removes the temporal channel–interference predictor and uses only the current observed channel and interference states for optimization. "w/o Priority" replaces the packet-priority score with a uniform weight, so urgent and ordinary packets are treated equally. "w/o Robust Margin" keeps the prediction module but removes the conservative uncertainty margins in Eq. (14), meaning that the optimizer directly uses predicted mean channel and interference values. "w/o Cross-layer Opt." removes the joint optimizer and replaces it with a decoupled heuristic that selects the channel, power, redundancy, and relay decisions separately.

To make the ablation results more visually comparable, Fig. 4 further reports the grouped-bar comparison of PDR, delay, energy consumption, and ISG. Each subfigure compares the full PCAO model with four ablated variants on DeepMIMO, RadioML, POWDER, and FlockLab.

As reported in Table 2 and visualized in Fig. 4, the full PCAO model consistently achieves the best performance across all datasets and metrics, confirming that the proposed modules are complementary rather than redundant. Removing cross-layer joint optimization causes the most severe degradation: on POWDER, PDR decreases from 95.2% to 88.9%, delay increases from 18.1 ms to 22.0 ms, energy consumption rises from 2.87 to 3.38 mJ/packet, and ISG drops from 6.94 dB to 5.57 dB. This indicates that jointly coordinating channel allocation, power control, redundancy, and relay preference is the core mechanism for balancing reliability, latency, energy, and anti-interference performance. Removing the prediction module also leads to clear performance loss, especially on POWDER and FlockLab, because the optimizer can no longer anticipate channel degradation or interference bursts before making transmission decisions. The variant without robust margin performs worse under interference-sensitive datasets, showing that conservative channel and interference estimation is necessary when the measured state is uncertain. The priority module has a relatively smaller but stable impact, because it mainly improves the protection of urgent or stale packets rather than all packets uniformly. Overall, PCAO performs best because it integrates predictive awareness, uncertainty robustness, packet-level importance modeling, and constrained cross-layer optimization into a single decision loop, enabling it to avoid unstable channels, suppress interference more effectively, reduce unnecessary energy expenditure, and maintain higher packet delivery reliability under heterogeneous transmission conditions.

5. Conclusion

This paper presented PCAO, a predictive cross-layer anti-interference optimization framework for IoT data transmission in unstable power-transmission environments. PCAO combines uncertainty-aware channel–interference prediction, packet-priority evaluation, robust state estimation, and constrained cross-layer optimization to jointly control channel allocation, transmission power, redundancy level, and relay preference. Experimental results on DeepMIMO, RadioML, POWDER, and FlockLab showed that PCAO consistently achieved superior packet delivery reliability, lower latency, higher interference suppression gain, and better energy efficiency than DQN, DDPG, PPO, and SAC. The ablation study further confirmed the contribution of each component and demonstrated the importance of integrating predictive modeling with cross-layer decision optimization. Although the current implementation relies on edge-assisted optimization and simplified communication assumptions, future research will focus on fully distributed deployment, adaptive online learning, and large-scale heterogeneous IoT scenarios. The proposed framework provides an effective and practical solution for reliable wireless transmission under dynamic interference and channel uncertainty.

References

[1] Liu H, Xiao L, Wang S, Lin W, Lv Z, Zhan Y, et al. Learning-Based Anti-Jamming Energy-Efficient Wide-Area Communications. IEEE Transactions on Wireless Communications. 2025;25:9830-43.

[2] Li J, Yang L, Hao W, Ahmad I, Liu H, Shu F, et al. Multi-layer transmitting RIS-aided receiver for collaborative jamming and anti-jamming networks. IEEE Transactions on Wireless Communications. 2025.

[3] Lin Z, Xiao L, Chen H, Lv Z, Zhu Y, Zhang Y, et al. Edge-assisted collaborative perception against jamming and interference in vehicular networks. IEEE Transactions on Wireless Communications. 2024;24(1):860-74.

[4] Li J, Xiao L, Wang C, Lv Z, Zhang P, Yang H. Learning-based energy-efficient anti-jamming fanet routing with qos guarantee. IEEE Transactions on Communications. 2025.

[5] Qin Y, Tang J, Tang F, Zhao M, Kato N. Multi-agent reinforcement learning in adversarial game environments: Personalized anti-interference strategies for heterogeneous UAV communication. IEEE Transactions on Mobile Computing. 2025.

[6] Asemian G, Amini M, Kantarci B. Anti-Jamming Task Scheduling in MEC-O-RAN with Hierarchical DRL and Transformer-Based Control. IEEE Internet of Things Journal. 2025.

[7] Zhang M, Xu X, Chu Z, Huang Y, Zhu Z, Cumanan K, et al. Improving Anti-Jamming Throughput for Wireless Powered IoT Networks: Is RIS Beneficial or Not? IEEE Internet of Things Journal. 2025.

[8] Zhu S, Ding Z, Chen J, Liang X, Wu Q, Jin R. Compact Time-Modulated Reconfigurable Antenna for Anti-Jamming IoT Communications. IEEE Internet of Things Journal. 2026.

[9] Wang H, Ouyang Q, Xi W, Xiang Y, Ye N. Dual Intelligence: Leveraging DRL With Smart Satellites to Counter Intelligent Jamming in Satellite Networks. IEEE Transactions on Cognitive Communications and Networking. 2025.

[10] Jing X, Wang R, Lei H, Liu H, Chen Q. Multi-Agent Discrete Soft Actor-Critic Algorithm-Based Multi-User Collaborative Anti-Jamming Strategy. IEEE Transactions on Information Forensics and Security. 2025;20:5025-38.

[11] Li L, Jing X, Lei H, Liang C, Chen Q. Distributed Anti-Jamming Strategy Based on Local Knowledge Diffusion and Differential Weighted Fusion Mechanisms. IEEE Transactions on Information Forensics and Security. 2025.

[12] Xu Y, Wang W, Li T. A communication confrontation based on the Stackelberg game: IRS aids for improving anti-jamming capability. IEEE Transactions on Green Communications and Networking. 2024;9(3):1280-93.

[13] Enwereonye UP, Shahraki AS, Alavizadeh H, Kayes A. Robust Multiuser Physical Layer Security for Grant-Free mMTC in Beyond 5G/6G Networks. IEEE Internet of Things Journal. 2025.

[14] Tuan BM, Nguyen DN, Trung NL, Nguyen VD, Van Huynh N, Hoang DT, et al. Securing MIMO Wiretap Channel with Learning-Based Friendly Jamming under Imperfect CSI. IEEE Internet of Things Journal.

2025;12(11):16009-22.
[15] Xiao L, Li J, Xiao Y, Lv Z, Wang C, Li P. Reinforcement Learning Based Accurate Worm Detection for Smart Grids. IEEE Internet of Things Journal. 2025.
[16] Niu Z, Yang H, Yao Q, Wu B, Yin S, Shen S, et al. Reliable low-latency routing for VLEO satellite optical network: A multiagent reinforcement learning approach. IEEE Internet of Things Journal. 2024;12(3):2309-21.
[17] Liu X, Zhou H, Zhang Z, Gao Q, Ma T. Multipath cooperative routing in ultradense LEO satellite networks: A deep-reinforcement-learning-based approach. IEEE Internet of Things Journal. 2024;12(2):1789-804.
[18] Liu J, Chen J, Liu Z, Zhou H. Enabling feedback-free MIMO transmission for FD-RAN: A data-driven approach. IEEE Transactions on Mobile Computing. 2024;24(3):2437-54.
[19] Xue J, Yuan D, Ma Z, Jiang T, Sun Y, Zhou H, et al. Large AI model for delay-doppler domain channel prediction in 6G OTFS-based vehicular networks. Science China Information Sciences. 2025;68(7):170306.
[20] Alkhateeb A. DeepMIMO: A Generic Deep Learning Dataset for Millimeter Wave and Massive MIMO Applications. arXiv preprint arXiv:190206435. 2019.
[21] O'Shea TJ, West N. Radio Machine Learning Dataset Generation with GNU Radio. In: Proceedings of the GNU Radio Conference. vol. 1; 2016. p. 1-5.
[22] O'Shea TJ, Corgan J, Clancy TC. Convolutional Radio Modulation Recognition Networks. In: Proceedings of the International Conference on Engineering Applications of Neural Networks. Springer; 2016. p. 213-26.
[23] Jacob R, Forno RD, Trüb R, Biri A, Thiele L. Dataset: Wireless link quality estimation on flocklab-and beyond. In: Proceedings of the 2nd Workshop on Data Acquisition To Analysis; 2019. p. 57-60.
[24] Mnih V, Kavukcuoglu K, Silver D, Rusu AA, Veness J, Bellemare MG, et al. Human-Level Control Through Deep Reinforcement Learning. Nature. 2015;518(7540):529-33.
[25] Lillicrap TP, Hunt JJ, Pritzel A, Heess N, Erez T, Tassa Y, et al. Continuous Control with Deep Reinforcement Learning. arXiv preprint arXiv:150902971. 2016.
[26] Schulman J, Wolski F, Dhariwal P, Radford A, Klimov O. Proximal Policy Optimization Algorithms. arXiv preprint arXiv:170706347. 2017.
[27] Haarnoja T, Zhou A, Abbeel P, Levine S. Soft Actor-Critic: Off-Policy Maximum Entropy Deep Reinforcement Learning with a Stochastic Actor. In: Proceedings of the 35th International Conference on Machine Learning. PMLR; 2018. p. 1861-70.